Journal of Molecular Structure 1033 (2013) 272–279

Contents lists available at SciVerse ScienceDirect

Journal of Molecular Structure

journal homepage: www.elsevier.com/locate/molstruc

Structural, spectroscopic (FT-IR, FT-Raman) and theoretical studies of the 1:1 cocrystal of isoniazid with *p*-coumaric acid

N. Ravikumar, Gopikrishna Gaddamanugu, K. Anand Solomon *

Department of Chemistry, Sankar Foundation Research Institute, Visakhapatnam 530 047, Andhra Pradesh, India

HIGHLIGHTS

- This research paper describes the experimental and theoretical studies on a co-crystal-which are usually prepared to enhance the physiochemical property of a molecule (usually an active pharmaceutical ingredient).
- Here the API is an anti-tuberculosis drug (Isoniazid) and the cocrystal former is a nutraceutical (*p*-coumaric acid). This combination can be termed as a "synergistic pharmaceutical co-crystal" as *p*-coumaric is sure to add its inherent anti-oxidant property, etc.
- Instead of using a GRAS listed compound (as a co-crystal former)- a molecule with well documented pharmacological property has been used. This can also be programmed in such a way that the side-effects of the API can be reduced by the co-crystal former.

ARTICLE INFO

Article history:
Received 19 July 2012
Received in revised form 6 October 2012
Accepted 9 October 2012
Available online 23 October 2012

Keywords:
API-nutraceutical
Cocrystal
X-ray crystallography
Ab initio

ABSTRACT

The 1:1 cocrystal of isoniazid (INH) with *p*-coumaric acid (*p*CA) has been prepared by slow evaporation method in methanol, which was crystallized in monoclinic $P2_1/n$ space group having four molecules in the asymmetric unit. The cocrystal has been characterized by single crystal X-ray analysis, FTIR, FT Raman and DFT calculations. The crystal structure was stabilized by O—$H_{phenol}\cdots N_{pyridine}$, N—H···O=C, COOH···N—H and C—H···O hydrogen bonding interactions. The geometry optimized structure of the cocrystal at the B3LYP/6-31G(d,p) level of theory has been used to calculate the vibrational frequencies.

1. Introduction

The physicochemical properties like stability and bioavailability play a major role in the development of an active pharmaceutical ingredient (API) into a drug candidate [1]. Often it is necessary to formulate an API into its corresponding salt or solvate for improved stability and bioavailability [2]. A cocrystal is a multicomponent molecular complex with definite stoichiometric ratio of two compounds that can interact through predominantly non-covalent interactions such as hydrogen bonding, π–π interactions and van der Waals forces [3]. A pharmaceutical cocrystal is a combination of an active pharmaceutical ingredient (API) with the GRAS (generally regarded as safe by US FDA) listed cocrystal former [4]. INH is a widely used drug alone in the prophylaxis and in combination with other anti-tuberculosis drugs in the treatment of all forms of tuberculosis [5]. Isoniazid proved to be a very potent and cost effective anti-tuberculosis drug, but Mycobacterium tuberculosis quickly becomes resistant when INH is administered as a single drug. This is the main reason why INH will always be used in combination with other anti-tuberculosis drugs [6]. In the recent years INH has drawn numerous attentions from the crystal engineering community due to its robust interactions with molecules having carboxylic acid groups to obtain pharmaceutical cocrystals [7]. INH has three pK_a values: pK_{a1} = 1.8 based on the hydrazine nitrogen, pK_{a2} = 3.5 based on the pyridine nitrogen and pK_{a3} = 10.8 based on the acidic group [8]. *p*CA is a hydroxy derivative of the cinnamic acid and naturally occurs in three isomers (ortho-, meta-, and para-); *p*CA is the most commonly occurring isomer in nature. *p*CA is found in various edible plants, such as peanuts, carrots, and tomatoes [9,10] and it is classified as a phytochemical nutraceutical. A number of promising pharmacokinetic studies have been conducted on *p*CA showing a positive response in protection against colon cancer on cultured mammalian cells [11] as well as antioxidant and anti-inflammatory properties in rats and rabbits [12–14]. *p*CA has two pK_a values: pK_{a1} = 4.6 based on the carboxylic acid oxygen and pK_{a2} = 9.3 based on the phenolic oxygen [15]. Herein we report the preparation, structural, vibrational and theoretical studies of the INH and *p*CA cocrystal.

* Corresponding author. Tel.: +91 9000888382.
E-mail address: anand.dcb@gmail.com (K. Anand Solomon).

0022-2860/$ - see front matter © 2012 Elsevier B.V. All rights reserved.
http://dx.doi.org/10.1016/j.molstruc.2012.10.029

2. Experimental

2.1. Synthesis

Both the starting materials INH and *p*CA were obtained from Sigma–Aldrich chemical suppliers. Analytical grade solvent was used for preparation of the cocrystal. The 1:1 mixture of INH (137 mg, 1 mmol) and *p*CA (164 mg, 1 mmol) was dissolved in 5 mL of methanol by heating at 60 °C. The obtained clear solution was filtered and slowly cooled to ambient temperature. The solvent was then allowed to evaporate at ambient temperature to obtain transparent yellow colored rectangular block crystals for 72 h.

2.2. Measurements

Single crystal X-ray diffraction measurements of the 1:1 cocrystal of INH with *p*CA (I) were carried out on Bruker axs kappa apex2 CCD Diffractometer with Mo Kα radiation at 293 K [16]. Data reduction was performed with the SAINT program [16] and the structure was solved using the SIR92 program [17]. SHELXL97 program was used for the refinement of the structure [18]. Structure-invariant direct methods were used for primary atom site locations and secondary atom site locations were found from the difference Fourier map. Hydrogen atom site locations were inferred from neighbouring sites. The final *R* factor is 0.036 by 2472 reflections and 211 refined parameters. The crystal data and the details of data processing are given in Table 1. The final fractional atomic coordinates listed in Table 2, bond lengths, bond angles and torsion angles are given in Table 3. The complete set of structural parameters in the CIF format is available from the Cambridge Crystallographic Database Center under No. CCDC 889545.

FTIR spectrum of I was recorded on a Bruker Alpha-T Fourier transform infrared spectrophotometer, using the KBr pellet method in the spectral range 4000–400 cm^{-1} with resolution of 2 cm^{-1} and the data were analyzed using the OPUS 6.5 software.

Table 1
Crystal data and structure refinement details for the 1:1 co-crystal of isoniazid with *p*-coumaric acid.

Empirical formula	$C_{15}H_{15}N_3O_4$
Formula weight	301.30
T (K)	293(2)
λ (Å)	0.71073
Crystal system	Monoclinic
Space group	$P2_1/n$
a (Å)	7.5750(3)
b (Å)	5.7100(2)
c (Å)	32.5700(5)
α (°)	90.00
β (°)	94.0450(10)
γ (°)	90.00
V (Å^3)	1405.25(8)
Z	4
D_x (g cm^{-3})	1.424
μ (mm^{-1})	0.106
F(000)	632
Crystal size (mm)	0.20 × 0.20 × 0.15
θ range for data collection (°)	2.5–30.4
Limiting indices	$-6 \leqslant h \leqslant 9$, $-6 \leqslant k \leqslant 6$, $-38 \leqslant l \leqslant 37$
Reflections collected/unique	12100/2472 [R(int) = 0.025]
Refinement method	Full-matrix least-squares on F^2
Data/restraints/parameters	2472/4/211
Goodness-of-fit on F^2	1.04
Final R indices [$I > 2\sigma(I)$]	R_1 = 0.0364, wR_2 = 0.0879
R indices (all data)	R_1 = 0.0443, wR_2 = 0.0942
Largest diff. peak and hole	0.15 and −0.22 e Å^{-3}
Data collection	Bruker APEX-II CCD
Data reduction	Bruker SAINT/XPREP
Structure solution	SIR92
Structure refinement	SHELXL97

Table 2
Atomic coordinates (×10^4) and equivalent isotropic displacement parameters (Å^2 × 10^3) for the 1:1 cocrystal of isoniazid with *p*-coumaric acid. U (eq) is defined as one third of the trace of the orthogonalized U_{ij} tensor.

Atom	x	y	z	U (eq)
C(1)	−452(10)	5333(14)	8583(2)	40(2)
C(2)	323(11)	3260(14)	8475(2)	44(2)
C(3)	1069(11)	1797(14)	8774(2)	43(2)
C(4)	1061(9)	2363(13)	9189(2)	37(2)
C(5)	257(10)	4462(14)	9289(2)	41(2)
C(6)	−495(10)	5922(14)	8993(2)	43(2)
C(7)	1868(10)	777(14)	9496(2)	41(2)
C(8)	2078(11)	1113(14)	9898(2)	43(2)
C(9)	2883(10)	−551(13)	10,193(2)	39(2)
C(10)	4709(10)	5151(14)	8653(2)	40(2)
C(11)	4930(10)	3846(14)	8262(2)	39(2)
C(12)	5827(12)	1769(15)	8231(3)	48(2)
C(13)	6000(13)	815(17)	7849(3)	57(2)
C(14)	4445(14)	3753(18)	7536(3)	62(3)
C(15)	4209(12)	4836(17)	7902(3)	55(2)
N(1)	5343(11)	1778(14)	7501(2)	58(2)
N(2)	5281(9)	4079(13)	9002(2)	41(2)
N(3)	5160(11)	5207(13)	9382(2)	45(2)
O(1)	−1210(8)	6843(11)	8302(2)	58(2)
O(2)	3217(8)	−2622(9)	10,044(2)	52(2)
O(3)	3224(8)	−54(10)	10,555(2)	50(2)
O(4)	4055(9)	7096(11)	8651(2)	60(2)
H(2)	342	2850	8199	53
H(3)	1589	402	8698	51
H(5)	230	4881	9565	50
H(6)	−1034	7307	9068	51
H(7)	2284	−636	9399	49
H(8)	1681	2524	10,000	51
H(12)	6311	1019	8466	58
H(13)	6614	−589	7833	68
H(14)	3946	4444	7296	75
H(15)	3570	6225	7909	65
H(1)	−1124	6322	8070	87
H(2B)	3666	−3454	10,229	77
H(2A)	5720(120)	2660(170)	9020(30)	60(30)
H(3A)	5660(110)	6630(140)	9360(30)	60(30)
H(3B)	4010(100)	5400(170)	9420(30)	70(30)

FT-Raman spectrum of I was recorded on a Bruker RFS 27, stand alone Fourier transform Raman spectrometer, using the KBr pellet method in the spectral range 4000–50 cm^{-1} with resolution of 2 cm^{-1}.

Tripos SYBYL expert molecular modeling environment was used to calculate the partition coefficient octanol/water (logP) of INH, *p*CA and I.

2.3. DFT calculations

The DFT calculations for the cocrystal I, were performed with the GAUSSIAN 03 program package [19]. The calculations employed the B3LYP exchange–correlation functional using 6-31G(d,p) basis set [20–23]. The single crystal X-ray geometry was used as a starting point for the optimization of the geometry of the cocrystal I. Both FTIR and FT Raman frequencies were calculated by the B3LYP/6-31G(d,p) level of theory. The calculated IR and Raman frequencies were positive and confirmed that the optimized structure is a local minimum on the potential energy hypersurface.

3. Results and discussion

3.1. Crystal structure

The 1:1 M ratio cocrystal I, was crystallized in monoclinic system with space group $P2_1/n$ with four molecules in the asymmetric unit. The structure of the cocrystal I with the atom numbering

Table 3
Bond lengths (Å), bond angles (°) and torsion angles for the 1:1 cocrystal of isoniazid with *p*-coumaric acid.

Parameters	X-ray	B3LYP/6-31G(d,p)
Bond lengths		
C(1)—O(1)	1.354(9)	1.379
C(1)—C(2)	1.378(11)	1.403
C(1)—C(6)	1.380(11)	1.405
C(2)—C(3)	1.375(11)	1.393
C(3)—C(4)	1.388(11)	1.412
C(4)—C(5)	1.394(11)	1.415
C(4)—C(7)	1.452(11)	1.458
C(5)—C(6)	1.368(11)	1.395
C(7)—C(8)	1.323(11)	1.354
C(8)—C(9)	1.454(11)	1.456
C(9)—O(3)	1.222(9)	1.242
C(9)—O(2)	1.309(9)	1.393
C(10)—O(4)	1.216(10)	1.266
C(10)—N(2)	1.335(10)	1.359
C(10)—C(11)	1.496(11)	1.493
C(11)—C(12)	1.374(11)	1.405
C(11)—C(15)	1.378(11)	1.403
C(12)—C(13)	1.374(12)	1.398
C(13)—N(1)	1.326(11)	1.351
C(14)—N(1)	1.326(13)	1.353
C(14)—C(15)	1.368(13)	1.396
N(2)—N(3)	1.404(9)	1.408
Bond angles		
O(1)—C(1)—C(2)	122.9(7)	122.18
O(1)—C(1)—C(6)	117.4(7)	117.75
C(2)—C(1)—C(6)	119.7(7)	120.06
C(3)—C(2)—C(1)	120.2(7)	119.41
C(3)—C(2)—H(2)	119.9	120.83
C(1)—C(2)—H(2)	119.9	119.75
C(2)—C(3)—C(4)	121.2(7)	121.66
C(2)—C(3)—H(3)	119.4	119.32
C(4)—C(3)—H(3)	119.4	119.01
C(3)—C(4)—C(5)	117.5(7)	117.10
C(3)—C(4)—C(7)	119.6(7)	118.85
C(5)—C(4)—C(7)	123.0(7)	123.44
C(6)—C(5)—C(4)	121.7(7)	121.20
C(6)—C(5)—H(5)	119.2	118.94
C(4)—C(5)—H(5)	119.2	119.84
C(5)—C(6)—C(1)	119.8(7)	119.95
C(5)—C(6)—H(6)	120.1	121.36
C(1)—C(6)—H(6)	120.1	118.68
C(8)—C(7)—C(4)	127.4(8)	127.35
C(8)—C(7)—H(7)	116.3	117.09
C(4)—C(7)—H(7)	116.3	115.54
C(7)—C(8)—C(9)	125.1(8)	123.72
C(7)—C(8)—H(8)	117.4	122.63
C(9)—C(8)—H(8)	117.4	113.63
O(3)—C(9)—O(2)	122.3(7)	120.75
O(3)—C(9)—C(8)	122.4(7)	125.20
O(2)—C(9)—C(8)	115.3(7)	114.04
O(4)—C(10)—N(2)	122.1(8)	122.15
O(4)—C(10)—C(11)	121.4(7)	120.53
N(2)—C(10)—C(11)	116.6(7)	117.35
C(12)—C(11)—C(15)	117.5(8)	118.29
C(12)—C(11)—C(10)	125.2(7)	123.59
C(15)—C(11)—C(10)	117.3(7)	118.09
C(11)—C(12)—C(13)	119.1(8)	118.80
C(11)—C(12)—H(12)	120.4	121.91
C(13)—C(12)—H(12)	120.4	119.23
N(1)—C(13)—C(12)	123.8(9)	123.12
N(1)—C(13)—H(13)	118.1	116.14
C(12)—C(13)—H(13)	118.1	120.72
N(1)—C(14)—C(15)	124.0(9)	123.07
N(1)—C(14)—H(14)	118.0	116.04
C(15)—C(14)—H(14)	118.0	120.87
C(14)—C(15)—C(11)	119.2(9)	118.94
C(14)—C(15)—H(15)	120.4	121.41
C(11)—C(15)—H(15)	120.4	119.64
C(13)—N(1)—C(14)	116.3(8)	117.74
C(10)—N(2)—N(3)	120.1(7)	123.98
C(10)—N(2)—H(2A)	125(6)	120.98
N(3)—N(2)—H(2A)	114(6)	115.02
N(2)—N(3)—H(3A)	108(6)	112.51
N(2)—N(3)—H(3B)	108(6)	111.85
H(3A)—N(3)—H(3B)	108(8)	111.94
C(1)—O(1)—H(1)	109.5	113.55
C(9)—O(2)—H(2B)	109.5	108.93
Torsion angles		
O(1)—C(1)—C(2)—C(3)	−179.9(8)	−177.82
C(6)—C(1)—C(2)—C(3)	−0.8(12)	−0.030
C(1)—C(2)—C(3)—C(4)	0.03(12)	0.101
C(2)—C(3)—C(4)—C(5)	0.5(12)	−0.091
C(2)—C(3)—C(4)—C(7)	−179.8(7)	179.86
C(3)—C(4)—C(5)—C(6)	−0.2(11)	0.011
C(7)—C(4)—C(5)—C(6)	−179.9(7)	179.94
C(4)—C(5)—C(6)—C(1)	−0.6(12)	0.058
O(1)—C(1)—C(6)—C(5)	−179.8(7)	179.88
C(2)—C(1)—C(6)—C(5)	1.1(12)	−0.049
C(3)—C(4)—C(7)—C(8)	175.2(8)	−179.59
C(5)—C(4)—C(7)—C(8)	−5.0(13)	0.358
C(4)—C(7)—C(8)—C(9)	179.3(7)	179.94
C(7)—C(8)—C(9)—O(3)	171.6(8)	−179.93
C(7)—C(8)—C(9)—O(2)	−8.3(12)	0.041
O(4)—C(10)—C(11)—C(12)	172.3(8)	156.45
N(2)—C(10)—C(11)—C(12)	−7.0(12)	−24.12
O(4)—C(10)—C(11)—C(15)	−6.1(12)	−22.45
N(2)—C(10)—C(11)—C(15)	174.5(7)	156.91
C(15)—C(11)—C(12)—C(13)	1.5(12)	−0.862
C(10)—C(11)—C(12)—C(13)	−176.9(8)	−179.76
C(11)—C(12)—C(13)—N(1)	−0.2(15)	−0.046
N(1)—C(14)—C(15)—C(11)	−0.2(15)	−0.616
C(12)—C(11)—C(15)—C(14)	−1.3(13)	1.173
C(10)—C(11)—C(15)—C(14)	177.2(8)	−179.86
C(12)—C(13)—N(1)—C(14)	−1.3(15)	0.627
C(15)—C(14)—N(1)—C(13)	1.5(15)	0.150
O(4)—C(10)—N(2)—N(3)	−0.84(12)	−1.799
C(11)—C(10)—N(2)—N(3)	178.6(7)	178.80

scheme is shown in Fig. 1. The aim of the present study is to compare the structural features in the crystal structure with the DFT optimized structure. The crystal was stabilized by intermolecular O—H···N, N—H···O hydrogen bonding interactions forming $R_2^2(7)$ ring motifs (Fig. 2). The phenolic OH group of *p*CA forms moderate hydrogen bonding [O(1)—H(1)···N(1) = 2.742(10) Å and <O(1)—H(1)—N(1) = 148.8°] with the nitrogen atom of the pyridine moiety of INH [24]. The amine nitrogen of INH also forms moderate hydrogen bonding, [N(3)—H(3A)···O(3) = 3.028(10) Å and <N(3)—H(3A)—O(3) = 169 (9)°] with the carboxylic acid's carbonyl group of *p*CA. But the carboxylic acid OH group of *p*CA forms weak hydrogen bonding [O(2)—H(2B)···N(2) = 3.338(9) Å and <O(2)—H(2B)—N(2) = 150.2°] with the amide nitrogen of INH [23]. The crystal structure is also stabilized by both inter and intra molecular C—H···O hydrogen bonding interactions forming $R_4^4(22)$ ring motifs (Fig. 3). The range of H···O distances (Table 4) found in I agrees with those found for C—H···O hydrogen bonds [25]. The crystal is also stabilized by van-der-Waals interactions. The crystal packing of I down the crystallographic *b*-axis is shown in Fig. 4.

3.2. B3LYP/6-31G(d,p) calculations

The DFT optimizations were performed on the X-ray structure I at B3LYP/6-31G(d,p) level which afforded the optimized structure (II) shown in Fig. 5. As evident from the results in Table 3, the bond lengths and bond angles of I and II correlate well. The angle between the planes defined by the aromatic ring atoms (N1C14C15C11C12C13) and (C3C4C5C6C1C2) in I is 4°, whereas in II the angle is 83° which is reflected in the variation of torsion angles of II listed in Table 3.

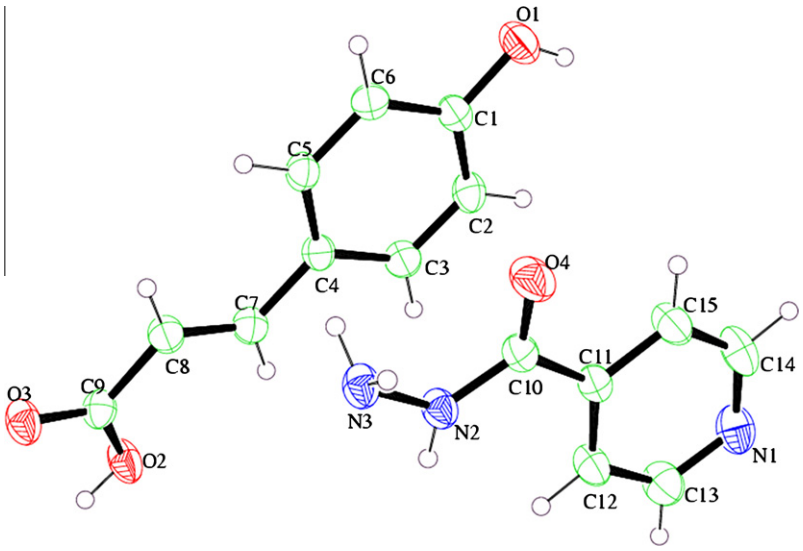

Fig. 1. Atom numbering scheme showing 50% probability displacement ellipsoids of the 1:1 cocrystal of isoniazid with *p*-coumaric acid.

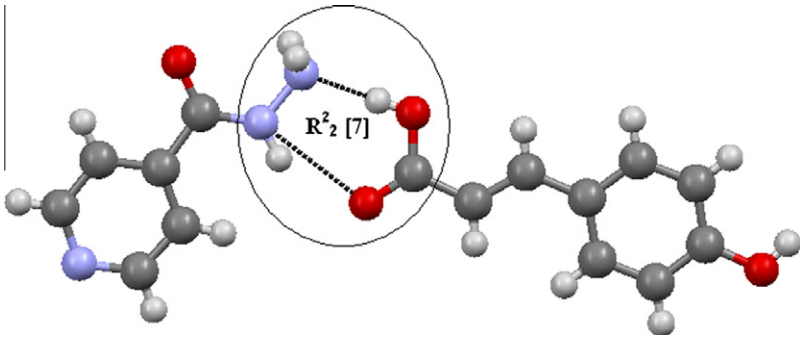

Fig. 2. Ring motif – R_2^2 [7] in the cocrystal.

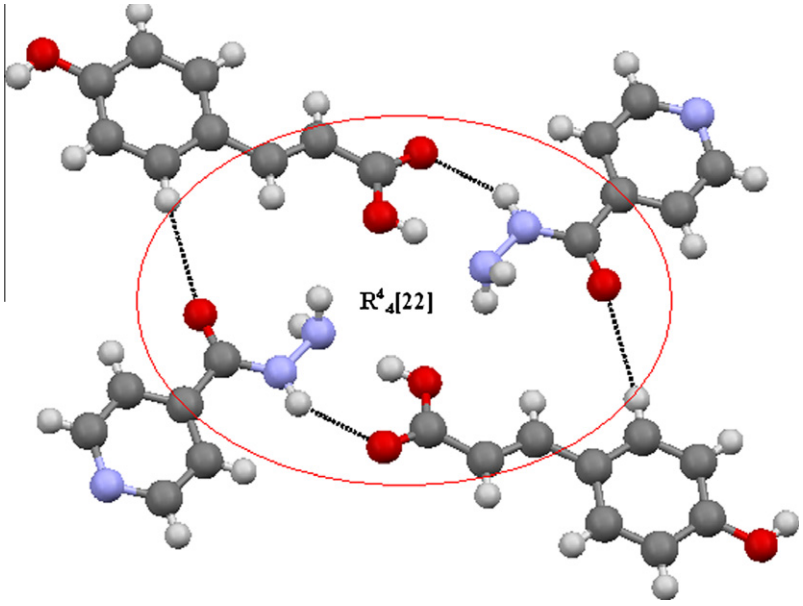

Fig. 3. Ring motif R_4^4 [22] in the cocrystal.

Table 4
Hydrogen bonds for the 1:1 co-crystal of isoniazid with *p*-coumaric acid (Å and °).

D—H···A	*d*(D—H)	*d*(H···A)	*d*(D···A)	<(DHA)
X-ray				
O(1)—H(1)···N(1)[a]	0.82	2.01	2.742(10)	148.8
N(2)—H(2A)···O(3)[b]	0.88(10)	2.15(10)	2.901(9)	144(8)
O(2)—H(2B)···N(2)[b]	0.82	2.60	3.338(9)	150.2
O(2)—H(2B)···N(3)[b]	0.82	1.80	2.619(9)	174.9
N(3)—H(3A)···O(3)[c]	0.90(7)	2.14(8)	3.028(10)	169(9)
N(3)—H(3B)···O(2)[d]	0.90(7)	2.43(9)	2.968(9)	119(7)
C(7)—H(7)···O(2)	0.93	2.45	2.7831	101

[a] Symmetry codes: $-x+1/2, y+1/2, -z+3/2$.
[b] Symmetry codes: $-x+1, -y, -z+2$.
[c] Symmetry codes: $-x+1, -y+1, -z+2$.
[d] Symmetry codes: $x, y+1, z$.

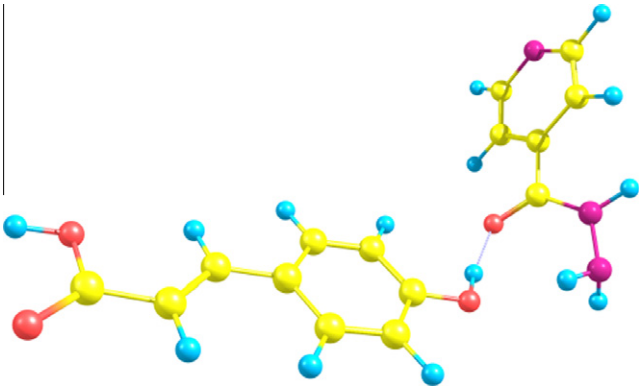

Fig. 5. The optimized structure at the B3LYP/6-31G(d,p) level of theory of the 1:1 cocrystal of isoniazid with *p*-coumaric acid.

3.3. Vibrational spectra

Fig. 6a shows the solid-state FTIR spectrum of the cocrystal I. The crystal structure analysis showed that both the phenolic–OH_{ar} and carboxylic acid–OH_{COOH} groups of *p*CA are involved in only intermolecular hydrogen bonds of 3.338(9), 2.742(10), 2.619(9) Å (Table 4). The νOH_{ar} band of *p*CA shifts from 3381 cm^{-1} to 3325 cm^{-1} due to an intermolecular hydrogen bonding with the pyridinium nitrogen atom of INH. The amide νNH band of INH shifts from 3304 cm^{-1} to 3285 cm^{-1}, due to hydrogen bonding interactions with the carbonyl group of the carboxylic acid of *p*CA. The broad absorption in the 1500–400 cm^{-1} region, with the centre of gravity at 1207 cm^{-1}, in the IR spectrum of I, arises from the stretching and bending vibrations of the OH groups, and it is characteristic of the short O—H···O hydrogen bonds [26]. No change was observed in the C=C stretching frequency at 1629 cm^{-1} of the styrene moiety of *p*CA in I.

The continuous absorption of the O—H···O vibrations in the 1500–400 cm^{-1} region overlaps bands assigned to in-plane and out-of-plane C—H, stretching and bending C—C, C—N, C—O vibrations, as well as the skeletal and ring ones. Some of these vibrations can be distinguished in the second-derivative (d^2) spectrum (Fig. 6b). The second-derivative (d^2) spectrum can be used to determine the frequencies of the narrow bands covered by the broad absorption due to the stretching and bending OHO vibrations. In the second-derivative (d^2) spectrum, the minima have the same wavenumbers as the maxima in the absorbance spectrum. The relative intensities of the bands in the d^2 spectrum vary inversely with the square of the half-width of the absorption bands [27,28].

The IR frequencies, calculated for II are shown in Fig. 6c as vertical lines. There are 105 modes in the 4000–0 cm^{-1} range and their intensities vary from 1609 to 0.005 km/mol. The proposed assignments of the IR bands are listed in Table 5. The most intense lines are assigned to the νN—H···O, ν(C=O), $\nu(CC)_{C=C}$, ν(C—OH), β(CH) and $\beta(CH)_{ar}$ vibrations. The experimental Raman spectrum of I, is shown in Fig. 7a. The Raman frequencies, calculated for II are shown in Fig. 7b as vertical lines. There are 105 modes in the 4000–0 cm^{-1} range and their intensities vary from 1411 to 0.005 km/mol. The tentative assignments of the Raman bands are listed in Table 6. In the Raman spectrum, the intensity of the νOH frequency is very weak [29] and the absorption due to νOH is absent. The spectrum shows strong absorption due to νC—H vibrations. The band assigned to the νC = O has weak intensity [30]. The IR frequency values obtained from the DFT calculations are very similar to those of the experimental values which did not require any further scaling [31].

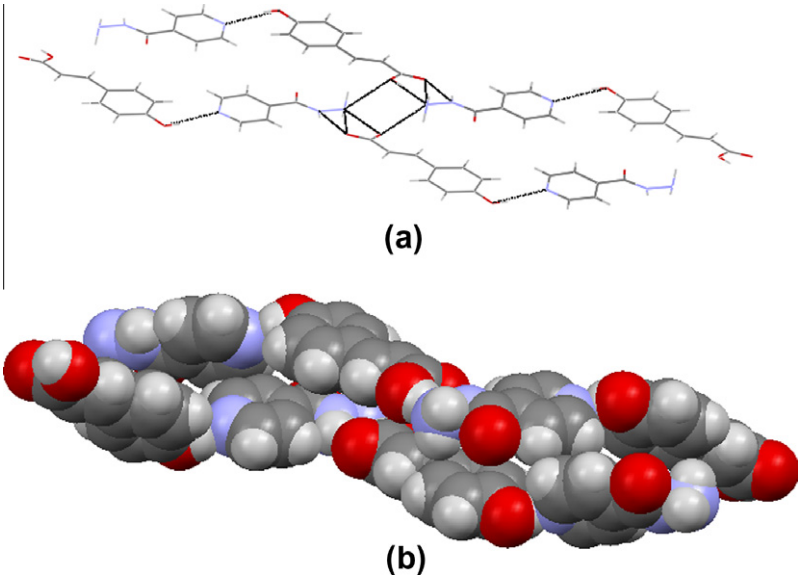

Fig. 4. The crystal packing diagram of the 1:1 cocrystal of isoniazid with *p*-coumaric acid down the crystallographic *b*-axis (a) two-dimensional view and (b) three-dimensional view.

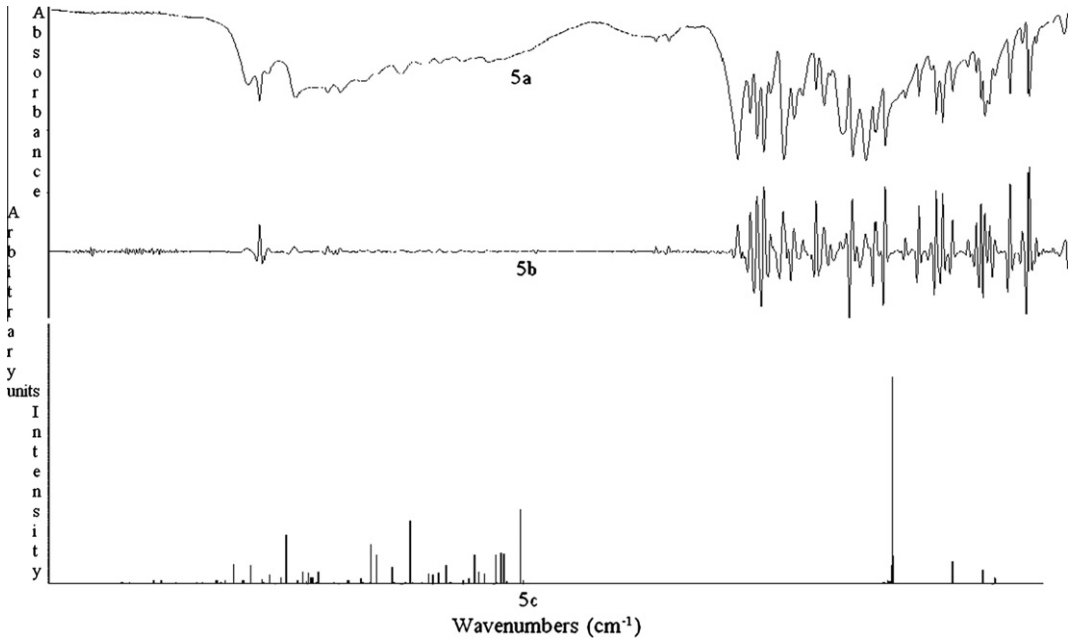

Fig. 6. Infrared spectra of the 1:1 cocrystal of isoniazid with *p*-coumaric acid, I (a) the experimental solid-state spectrum of I, (b) the second-derivative spectrum of I, and (c) IR frequencies calculated by the B3LYP/6-31G(d,p) approach for II.

Table 5
FTIR experimental (ν_{exp}), second derivative (d^2) and calculated (ν_{cal}) by the B3LYP/6-31G(d,p) frequencies (cm^{-1}) for the 1:1 cocrystal of isoniazid with *p*-coumaric acid.

I		II		
ν_{exp}	d^2	ν_{cal}	Intensity[a]	Assignments[b]
		3470	169.21	νO—H$_{ar}$···N
3325	3326			νN—H···O=C
3285	3286	3250	2.70	νN—H···O=C
		3236	217.36	νN—H···O=C
		3233	1609.8	νN—H···O=C
		3229	19.33	νN—H···O=C
		3226	146.14	νN—H···O=C
		3219	25.02	νN—H···O=C
3059		3195	15.99	νCH$_{ar}$ + νCH$_{C=C}$
3017		3190	0.02	νCH$_{ar}$ + νCH$_{C=C}$
1672	1672	1671	236.35	ν(C=O)
		1656	240	ν(C=O)
		1639	15.92	ν(C=O)
1629	1629	1631	231.55	ν(CC)$_{C=C}$
1605	1606	1592	82.84	ν(CC)$_{ar}$
1582	1583	1571	97.02	ν(CC)$_{ar}$
1560	1562	1553	222.92	ν(CN)$_{ar}$, β(H—N—N)
1514	1518	1527	44.34	ν(CC)$_{ar}$
1479	1481	1502	32.55	β(C—N—H)
1450	1450	1453	12.30	β(CH)$_{C=C}$
		1433	144.51	β(CH)$_{C=C}$
1408	1409	1405	93.30	ν(CC)$_{ar}$
1380	1382	1377	74.42	β(CH)$_{C=C}$ + β(OH)$_{ar}$
		1360	81.25	β(CH)$_{C=C}$ + β(OH)$_{ar}$
		1350	2.28	β(CH)$_{C=C}$ + β(OH)$_{ar}$
		1332	12.26	β(CH)$_{C=C}$ + β(OH)$_{ar}$
1317	1317	1324	1.58	νC—N
1283	1285	1295	7.68	ν(C—OH)
		1285	479.06	ν(C—OH)
		1267	10.75	ν(C—OH)
		1265	0.42	ν(C—OH)
1238	1239	1230	9.95	β(OH)$_{ar}$
1207	1208	1225	129.01	β(CH)
1175	1176	1164	229.34	β(CH)$_{ar}$
		1145	297.16	β(CH)$_{ar}$
		1135	7.05	β(CH)$_{ar}$
1106	1106	1109	20.26	β(CH)
		1101	40.51	β(CH)
1002	1002	1048	30.48	β(CH)
		1046	1.21	β(CH)
		1031	0.76	β(CH)
		1013	0.80	β(CH)
		1005	2.24	β(CH)
980	980	993	1.47	ν(CCO)
		988	10.60	ν(CCO)
946	947	927	10.05	γ(CH)$_{ar}$
920	922	922	98.52	γ(CO)
		916	7.28	γ(CO)
		902	48.48	γ(CO)
848	849	886	91.49	γ(CH)
		879	4.69	γ(CH)
		874	21.51	γ(CH)
		865	96.48	γ(CH)
		848	27.40	γ(CH)
836	837	819	6.66	γ(CH)$_{ar}$
750	750	798	377.41	α(CCC)
		779	48.73	α(CCC)
		756	1.13	α(CCC)
		727	68.02	α(CCC)
687	687	693	0.38	β(CO)
		672	1.73	β(CO)
		650	153.52	ø(CO)
		553	30.99	γOH
		524	27.69	α(C=CC)
		437	9.92	β(CH)
		435	0.12	β(CH)
		329	2.30	γ(OH)$_{ar}$

ν – Stretching; β – deformation in-plane; γ – deformation out-of-plane; α(CCC) – aromatic ring in-plane deformation: ø – aromatic ring out-of-plane deformation.
[a] Intensity in km/mol.
[b] Assignments for calculated frequencies for II.

3.4. LogP calculations

The logP calculated by Tripos SYBYL expert molecular modeling environment for the cocrystal I, is found to be 0.82, where as for

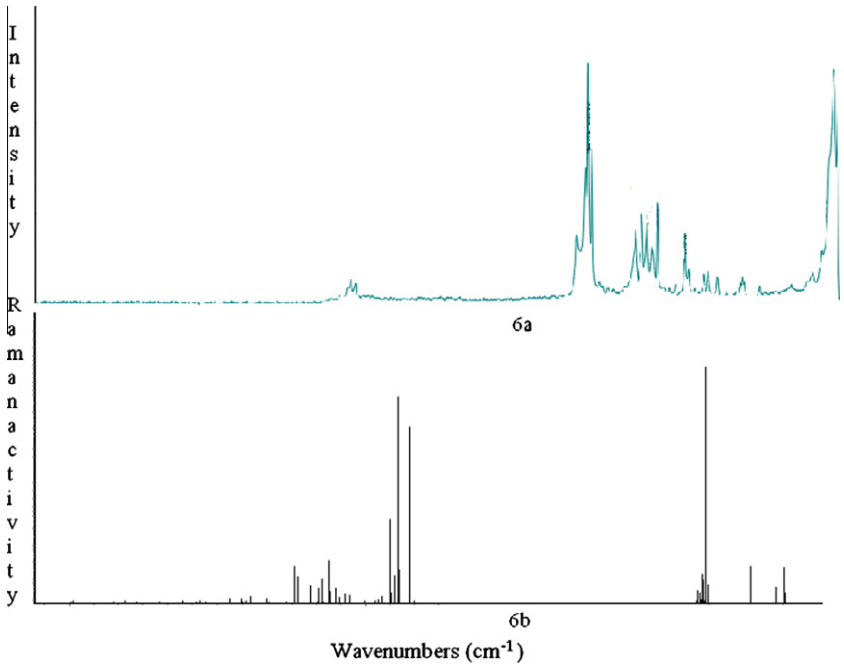

Fig. 7. Raman spectra of the 1:1 cocrystal of isoniazid with *p*-coumaric acid, I (a) the experimental solid-state spectrum of I and (b) Raman frequencies calculated by the B3LYP/6-31G(d,p) approach for II.

Table 6
Raman experimental (R_{exp}) and calculated (R_{cal}) by the B3LYP/6-31G(d,p) frequencies (cm^{-1}) for the 1:1 cocrystal of isoniazid with *p*-coumaric acid.

I	II		
R_{exp}	R_{cal}	Intensity[a]	Assignments[b]
	3233	1411.49	νN—H···O
3060	3195	79.60	$\nu CH_{ar} + \nu CH_{C=C}$
	3190	13.51	$\nu CH_{ar} + \nu CH_{C=C}$
3025			$\nu CH_{ar} + \nu CH_{C=C}$
1673	1671	1236.13	ν(C=O)
1624	1656	168.07	$\nu(CC)_{C=C}$
	1639	65.96	$\nu(CC)_{C=C}$
1607	1631	503.23	$\nu(CC)_{ar}$
	1592	38.42	$\nu(CC)_{ar}$
1585	1571	25.47	$\nu(CC)_{ar}$
	1553	15.3	β(H—N—N)
	1527	5.34	$\nu(CC)_{ar}$
	1502	12.39	β(C—N—H)
1319	1350	4.50	$\beta(CH)_{C=C} + \beta(CH)_{ar}$
	1332	71.42	$\beta(CH)_{C=C} + \beta(CH)_{ar}$
	1324	261.55	$\beta(CH)_{C=C} + \beta(CH)_{ar}$
1273	1285	147.81	ν(C—OH)
	1267	89.93	ν(C—OH)
	1265	89.98	ν(C—OH)
1239	1230	54.13	$\beta(OH)_{ar}$
1206	1225	103.64	β(CH)
1174	1164	161.01	$\beta(CH)_{ar}$
	1145	224.98	$\beta(CH)_{ar}$
	1135	1.26	$\beta(CH)_{ar}$
1003	1031	1.55	β(CH)
	1013	8.10	β(CH)
	1005	31.68	β(CH)
983	988	5.57	ν(CCO)
	993	0.40	ν(CCO)
893	916	4.55	$\beta(CNC)_{ring}$
	902	21.20	$\beta(CNC)_{ring}$
	886	9.70	$\beta(CNC)_{ring}$
862	879	26.76	γ(CH)
	874	3.34	γ(CH)
	865	2.58	γ(CH)
804	848	3.63	$\gamma(CH)_{ar}$
	819	30.19	$\gamma(CH)_{ar}$
	798	3.99	α(CCC)
	693	6.95	β(CC=O)
	672	12.01	β(CC=O)
652	650	8.02	ø(CC)
	624	4.34	α(CCC)
	553	2.41	γOH
	531	0.25	α(C=C—C)
	524	0.48	ø(CC)
	463	8.49	ø(CC)
	437	1.06	β(CH)
	435	0.24	β(CH)
	329	4.16	$\gamma(OH)_{ar}$

ν – Stretching; β – deformation in-plane; γ – deformation out-of-plane; α – aromatic ring in-plane deformations; ø – aromatic ring out-of-plane deformations.
[a] Intensity in km/mol.
[b] Assignments for calculated frequencies for II.

INH and *p*CA the logP values are −0.6680 and 1.5720. As INH is too hydrophilic (negative logP) it is unable to pass through membranes, as they hardly enter the hydrophobic interior of the lipophilic bilayer. Whereas *p*CA is too lipophilic (high logP) it poorly permeates through membranes. Since the cocrystal I, has moderate logP value it is neither too hydrophobic nor too lipophilic it would be able to pass through the lipophilic bilayer [32,33].

4. Conclusions

The crystal structure of the 1:1 cocrystal of INH with *p*CA is stabilized by $O—H_{phenol}\cdots N_{pyridine}$, N—H···O=C and COOH···N—H hydrogen bonding interactions. The crystal structure is also stabilized by both intra and intermolecular C—H···O hydrogen bonds. In the optimized structure of I, estimated by the B3LYP/6-31G(d,p) level of theory, the angle between the approximate planes of the two molecules in the cocrystal is deviated by 80°

from the crystal structure of I. In the cocrystal I, the IR bands for INH amine (NH_2) group are observed at 3285 cm^{-1} ($_{asym}NH_2$) and 3167 cm^{-1} ($_{sym}NH_2$) which are shifted from 3304 cm^{-1} to 3112 cm^{-1} respectively due to hydrogen bonding interactions with the COOH group of *p*CA. In the FTIR spectrum the absorption frequencies in the 3325–3285 cm^{-1} region confirms the presence of the hydroxyl groups involved in moderate hydrogen bonding interactions. In the Raman spectrum a medium band at 1673 cm^{-1} is observed due to C=O stretching vibrations. The strong bands at 1624 cm^{-1} and 1607 cm^{-1} are assigned due to ring $C{=}N_{asym}$ and ring $C{=}C_{asym}$ stretching vibrations.

Acknowledgements

The authors thank the Managing Trustee and the Founder Trustee of the Sankar Foundation for their financial support and encouragement. We thank Dr. Chelli Janardhana, Head of the Chemistry department, Sri Sathya Sai University, Puttaparthi, Andhra Pradesh, for the usage of Gaussian software. We also thank the DST and SAIF, IIT Madras for the single crystal X-ray data collection and FT Raman analysis.

References

[1] I. Kola, J. Landis, Nat. Rev. Drug Discovery 3 (2004) 711.
[2] S.R. Byrn, R.R. Pfeiffer, G. Stepenson, D.J.W. Grant, W.B. Gleason, Chem. Mater. 6 (1994) 1148.
[3] G.P. Stahly, Cryst. Growth Des. 9 (2009) 4212.
[4] P. Vishweshwar, J.A. McMahon, J.A. Bis, M.J. Zaworotko, J. Pharm. Sci. 95 (2006) 499.
[5] USP DI®, Drug Information for the Health Care Professional, 15th ed., vol. I, 1995, pp. 1627.
[6] Y.L. Janin, Bioorg. Med. Chem. 15 (2007) 2479.
[7] A. Lemmerer, J. Bernstein, V. Kahlenberg, Cryst. Eng. Comm. 12 (2010) 2856.
[8] N.F. Atta, A. Galal, R.A. Ahmed, Int. J. Electrochem. Sci. 6 (2011) 5097.
[9] S.T. Talcott, C.E. Duncan, D.D. Pazo-Insfran, D.W. Gorbet, Food Chem. 89 (2005) 77.
[10] M.P. Kahkonen, A.I. Hopia, H.J. Vuorela, J.P. Rauha, K. Pihlaja, T.S. Kujala, M. Heinonen, J. Agric. Food Chem. 47 (1999) 3954.
[11] L.R. Ferguson, Z. Shou-tun, P.J. Harris, Mol. Nutr. Food Res. 49 (2005) 585.
[12] C. Luceri, L. Giannini, M. Lodovici, E. Antonucci, R. Abbate, E. Masini, P. Dolara, Br. J. Nutr. 97 (2007) 458.
[13] F. Guglielmi, C. Luceri, L. Giovannelli, P. Dolara, M. Lodovici, Br. J. Nutr. 89 (2003) 581.
[14] C. Luceri, F. Guglielmi, F. Meoni, P. Dolara, Scand. J. Gastroenterol. 39 (2004) 1128.
[15] J.L. Beltran, N. Sanli, G. Fonrodona, D. Barron, G. Özkan, J. Barbosa, Anal. Chim. Acta 484 (2003) 253.
[16] Bruker APEX2, SAINT and SADABS, Bruker AXS Inc., Madison, Wisconsin, USA, 2004.
[17] A. Altomare, G. Cascarano, C. Giacovazzo, A. Guagliardi, J. Appl. Cryst. 26 (1993) 343.
[18] G.M. Sheldrick, Acta Cryst. A64 (2008) 112.
[19] M.J. Frisch, G.W. Trucks, H.B. Schlegel, G.E. Scuseria, M.A. Robb, J.R. Cheeseman, J.A. Montgomery, Jr., T. Vreven, K.N. Kudin, J.C. Burant, J.M. Millam, S.S. Iyengar, J. Tomasi, V. Barone, B. Mennucci, M. Cossi, G. Scalmani, N. Rega, G.A. Petersson, H. Nakatsuji, M. Hada, M. Ehara, K. Toyota, R. Fukuda, J. Hasegawa, M. Ishida, T. Nakajima, Y. Honda, O. Kitao, H. Nakai, M. Klene, X. Li, J.E. Knox, H.P. Hratchian, J. B. Cross, V. Bakken, C. Adamo, J. Jaramillo, R. Gomperts, R.E. Stratmann, O. Yazyev, A.J. Austin, R. Cammi, C. Pomelli, J.W. Ochterski, P.Y. Ayala, K. Morokuma, G.A. Voth, P. Salvador, J.J. Dannenberg, V.G. Zakrzewski, S. Dapprich, A.D. Daniels, M.C. Strain, O. Farkas, D.K. Malick, A.D. Rabuck, K. Raghavachari, J.B. Foresman, J.V. Ortiz, Q. Cui, A.G. Baboul, S. Clifford, J. Cioslowski, B.B. Stefanov, G. Liu, A. Liashenko, P. Piskorz, I. Komaromi, R.L. Martin, D.J. Fox, T. Keith, M.A. Al-Laham, C.Y. Peng, A. Nanayakkara, M. Challacombe, P.M.W. Gill, B. Johnson, W. Chen, M.W. Wong, C. Gonzalez, J.A. Pople, GAUSSIAN 03, Revision C.02, Gaussian, Inc., Wallingford, CT, 2004.
[20] A.D. Becke, J. Chem. Phys. 98 (1993) 5648.
[21] A.D. Becke, J. Chem. Phys. 107 (1997) 8554.
[22] C. Lee, W. Yang, G.R. Parr, Phys. Rev. B 37 (1988) 785.
[23] W.J. Hehre, L. Random, P.V.R. Schleyer, J.A. Pople, Ab Initio Molecular Orbital Theory, Wiley, New York, 1986.
[24] G.A. Jeffrey, H. Maluszynska, J. Mitra, Int. J. Biol. Macromol. 7 (1985) 336.
[25] G.R. Desiraju, T. Steiner, The Weak Hydrogen Bond, University Press, Oxford, 1999.
[26] D. Hadzi, S. Bratos, P. Schuster, G. Zundel, C. Sandorfy (Eds.), Hydrogen Bond: Recent Developments in Theory and Experiments, vol. 2, Springer, Amsterdam, 1976, p. 565.
[27] W.F. Maddams, M.J. Southon, Spectrochim. Acta 38A (1992) 459.
[28] G. Talsky, Derivative Spectrophotometry, VCR, Weinheim, 1994.
[29] B. Schrader (Ed.), Infrared and Raman Spectroscopy: Methods and Applications, VCH, Weinheim, 1995.
[30] E. Smith, G. Dent, Modern Raman Spectroscopy: A Practical Approach, Wiley & Sons Ltd., Chichester, 2005.
[31] Z. Dega-Szafran, G. Dutkiewicz, Z. Kosturkiewicz, M. Szafran, J. Mol. Struct. 889 (2008) 286.
[32] M. Newcomb, S. Moore, D. Cram, J. Am. Chem. Soc. 99 (1977) 6405.
[33] C. Hansch, J. Org. Chem. 43 (1978) 4889.